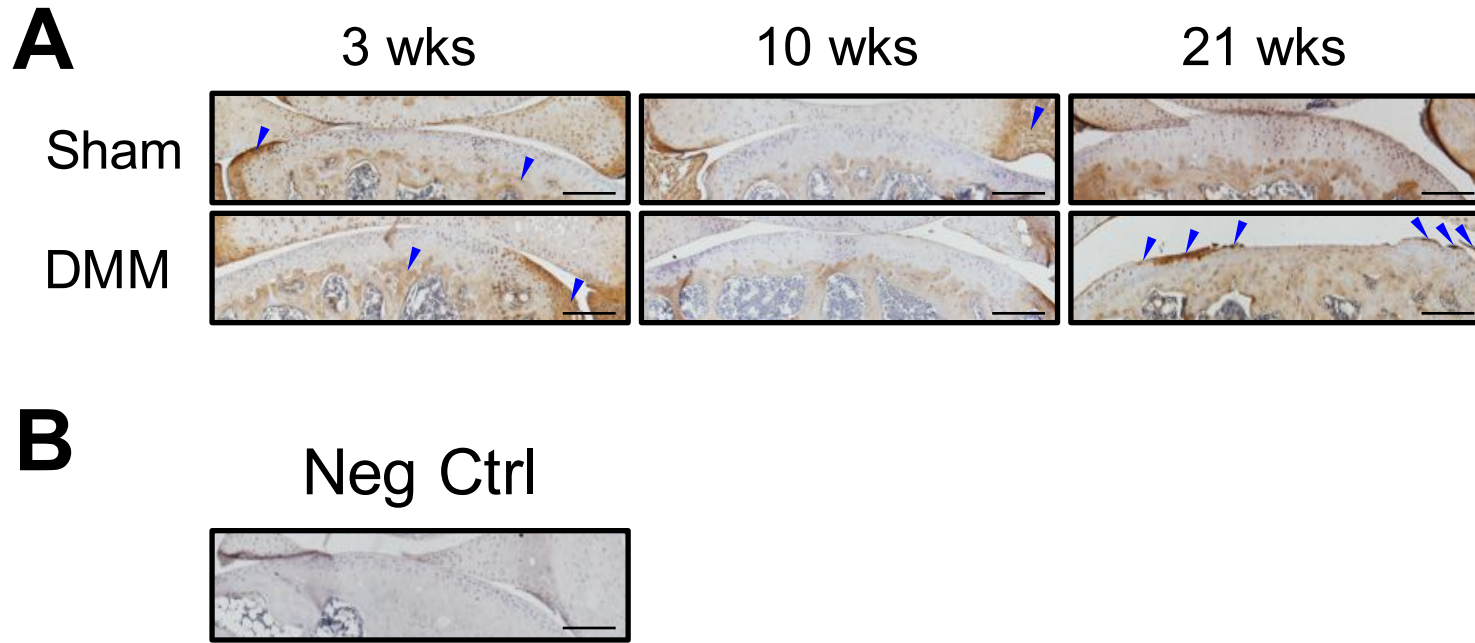
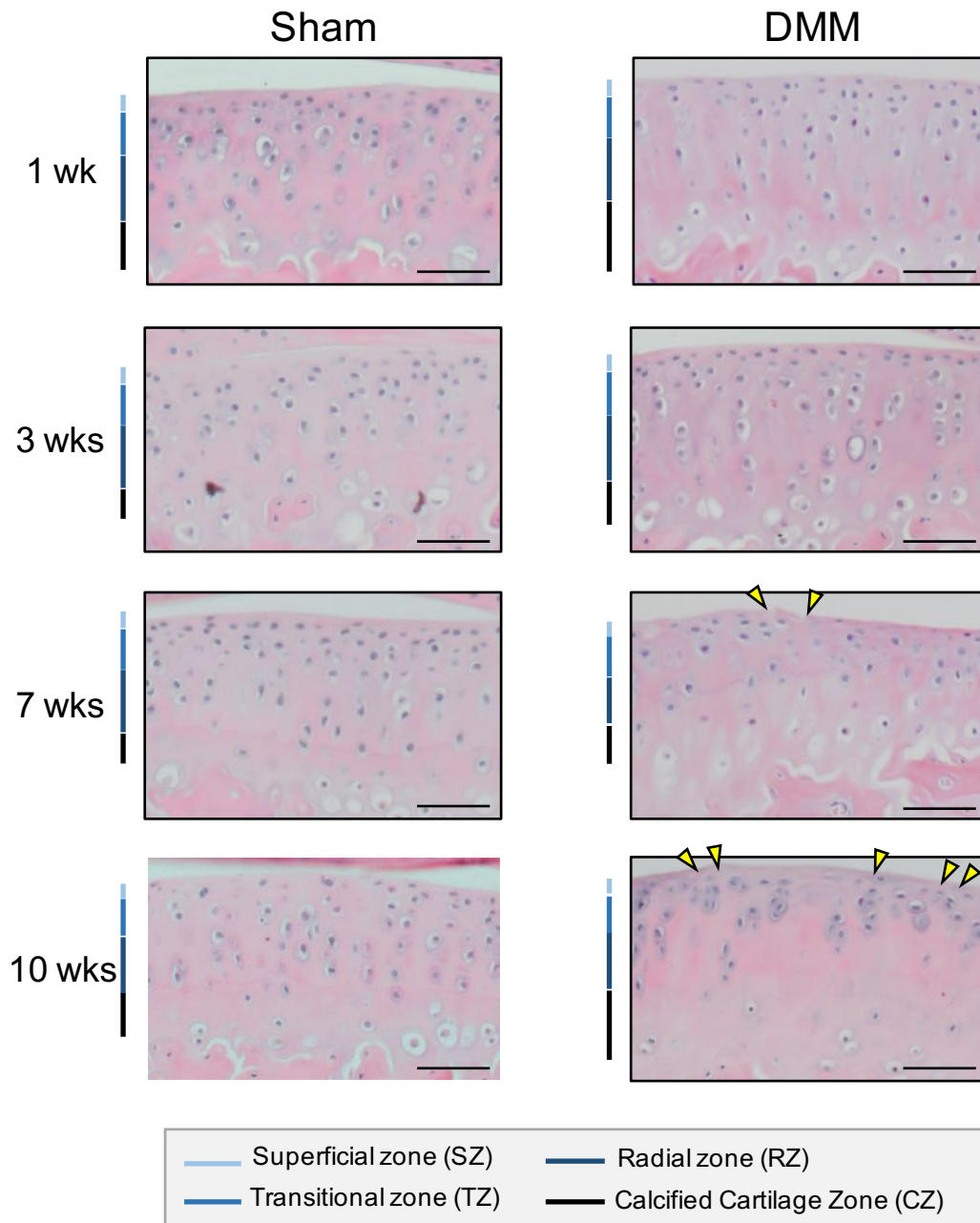


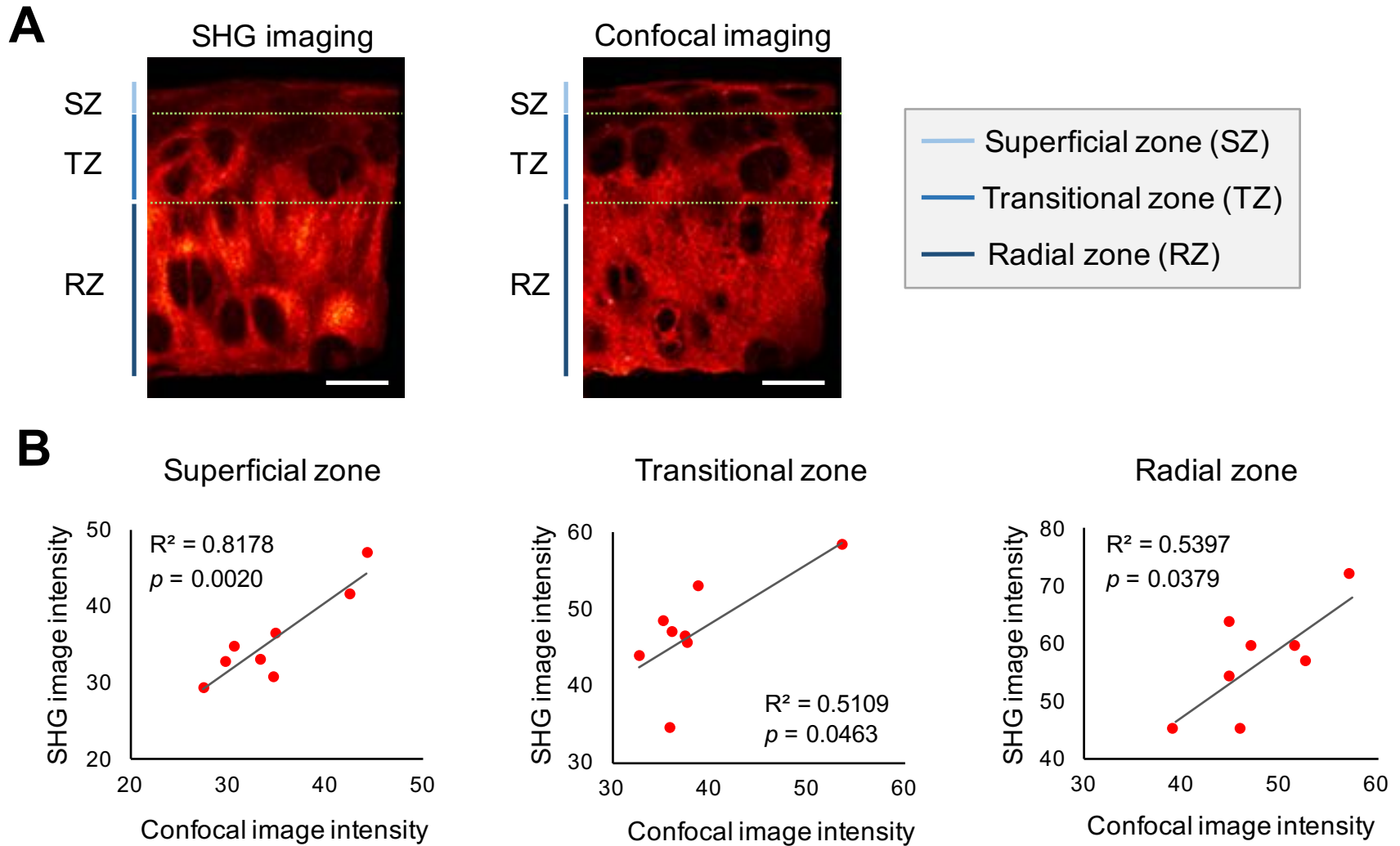
Supplemental Figure 1. Negative control for Collagen II immunofluorescence staining. As a negative control for Collagen II immunofluorescence staining, sections were incubated with the secondary antibody only: goat anti-rabbit antibody Alexa 594. A) No fluorescence signal (red) was detected in the articular cartilage of the femur and tibia. Autofluorescence was detected in the bone marrow of the subchondral bone (arrowheads). B) DAPI was used to indicate nuclei. C) An overlay of images from A and B. Scale bars = 400 μ m.



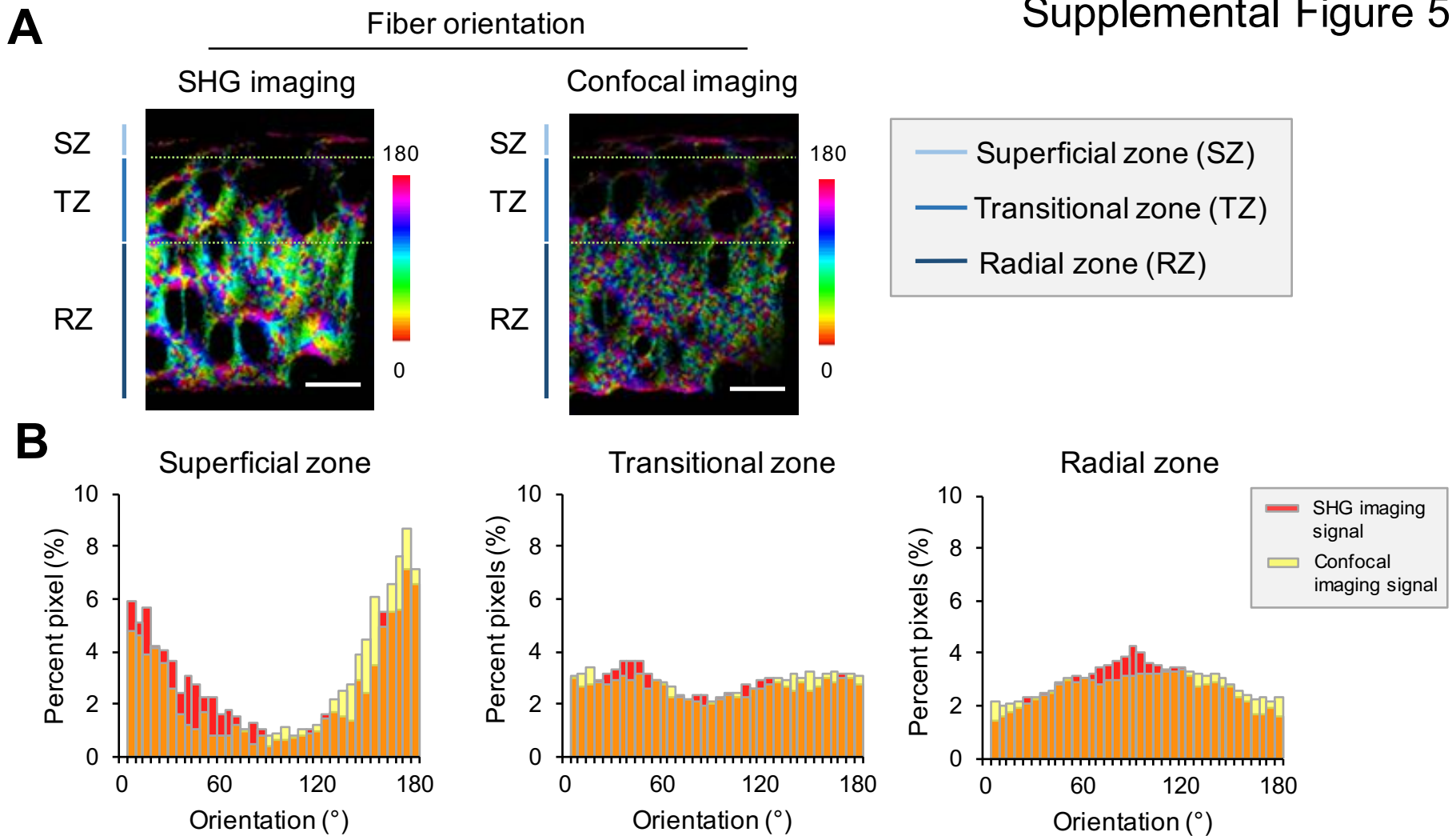
Supplemental Figure 2. IHC analysis detecting collagen I protein levels in knee joints of NFkB luciferase reporter mouse post-OA induction. A) IHC images of collagen I protein on sections from mouse knee joints at 3-, 10-, and 21-weeks post-DMM or Sham surgery. Arrowheads indicate positive staining in the subchondral bone, areas in the lateral meniscus, and areas lateral to the articular surface. Only articular cartilage from 21-weeks post-surgery samples had positive collagen I staining in the articular cartilage. B) Sections from 21-weeks post-surgery mice with no primary antibody served as a negative control. Scale bar = 200 μ m.



Supplemental Figure 3. Hematoxylin and Eosin (H&E) stained samples of mouse articular cartilage at 1-, 3-, 7-, and 10-weeks post-surgery. Superficial, transitional, radial, and calcified cartilage zones were present in samples at all the times post-DMM and Sham surgeries. Arrowheads: fibrillation in articular surface in the DMM samples. Scale bar = 50 μ m.



Supplemental Figure 4. Comparison of signal intensity from SHG and confocal imaging of sections after collagen II immunofluorescence staining. A) Images of SHG and confocal imaging. Superficial, transitional and radial zones were delineated. Scale bars = 50 μ m. B) Correlation analysis of image intensity from SHG imaging and confocal imaging. Good correlation in all zones of articular cartilage were found. $p < 0.05$ indicates significant correlation between imaging modalities.

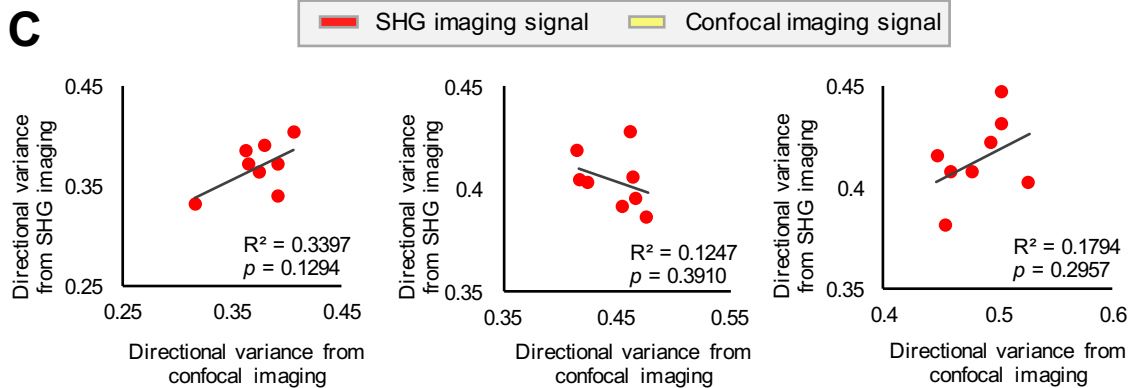
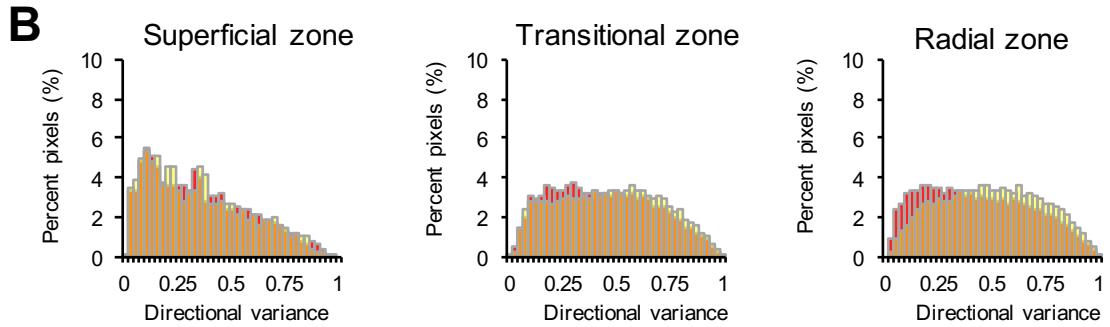
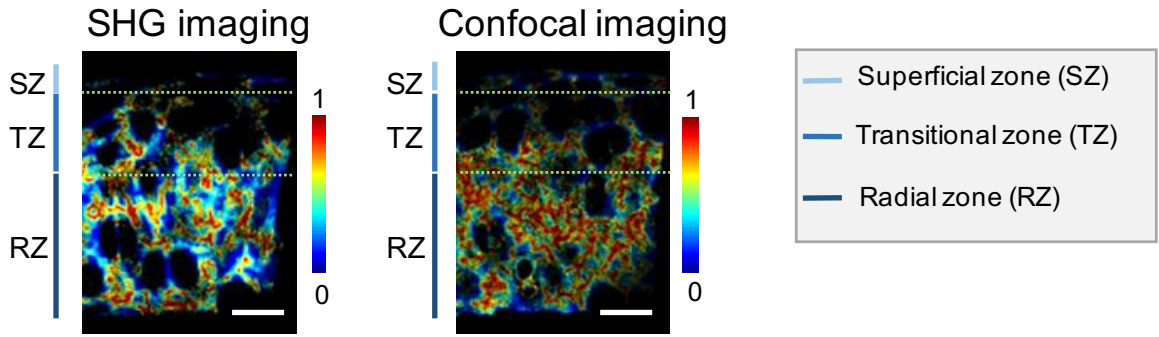


Supplemental Figure 5. Comparison of collagen fiber alignment from SHG imaging and confocal microscopy on samples stained with an anti-collagen II antibody. A) Heat maps of fiber orientation in reference to the articular cartilage surface were generated. Both confocal and SHG imaging revealed more collagen fiber signals lying parallel to the articular surface (toward 0 and 180°, red hues) in the superficial zone, and more collagen fiber orientation exhibited random distribution in the transitional zone. Scale bars = 50 μ m. B) Quantification of collagen fiber orientation in the superficial, transitional, and radial zones of the cartilage from the SHG (red bars) and confocal (yellow bars) imaging. Similar, but not identical trends of fiber orientation from the two imaging modalities were found in all zones. In the radial zone, SHG imaging identified a peak at around 90° (i.e. indicating perpendicular orientation of the fibers), whereas confocal imaging only identified a plateau with broad range (from about 50° to 150°).

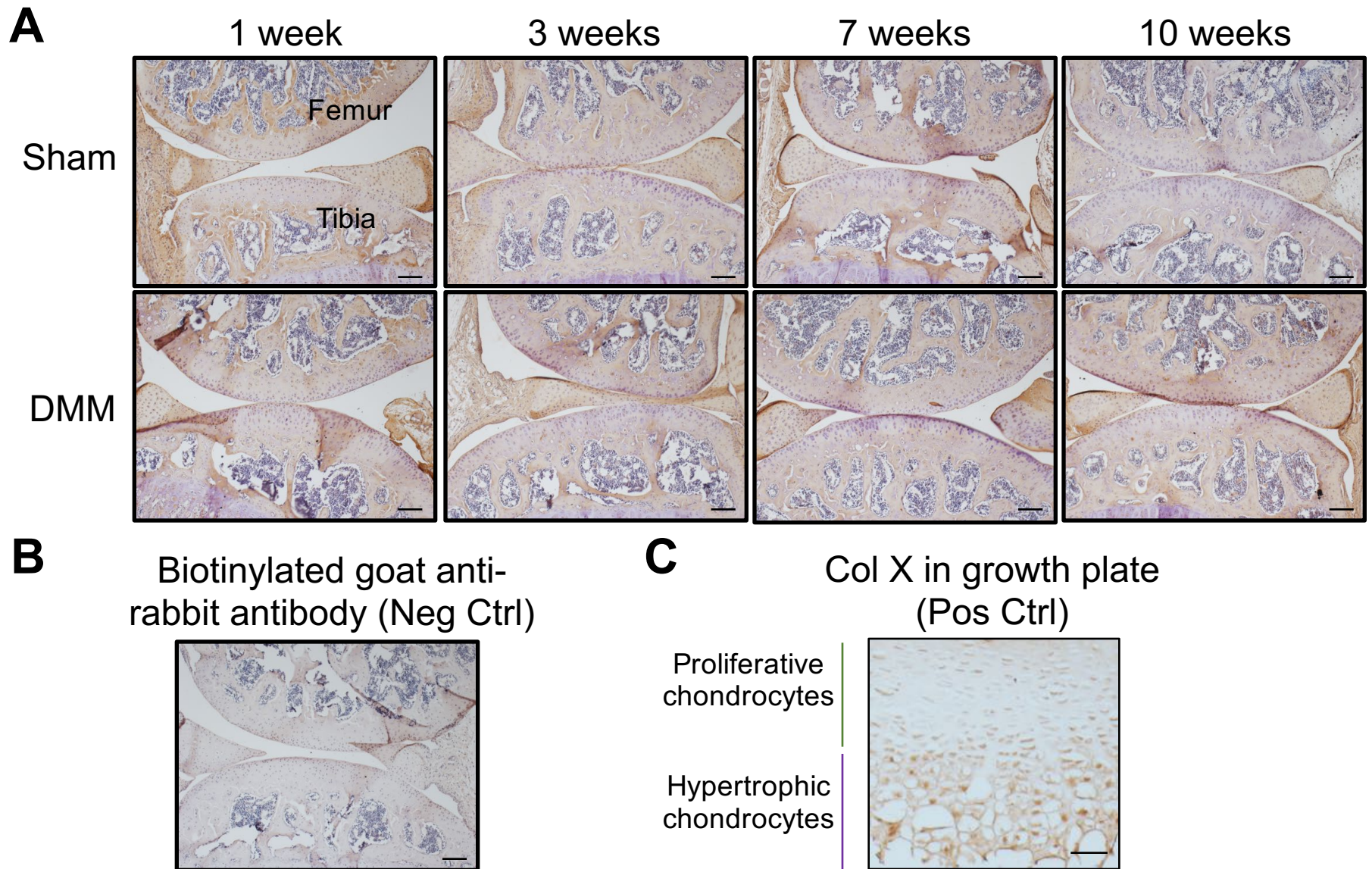
A

Directional Variance

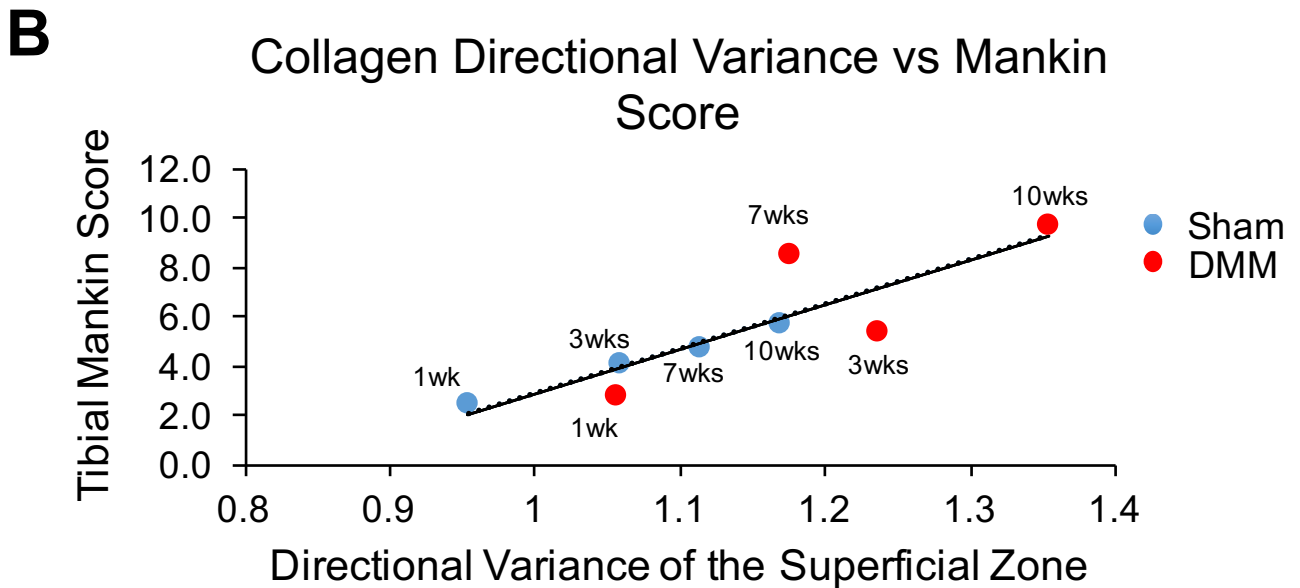
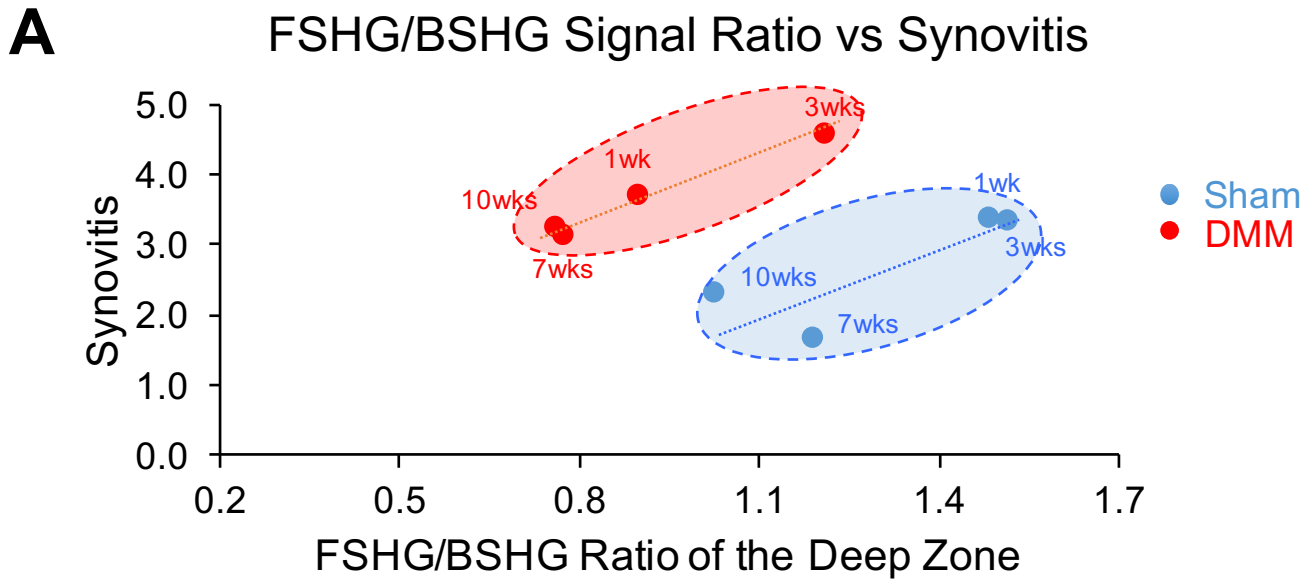
Supplemental Figure 6



Supplemental Figure 6. Directional variance analysis of collagen fibers from SHG and confocal imaging on anti-collagen II stained samples. A) Based on fiber orientation heat maps from SHG and confocal imaging, the directional variance was calculated, which reflects the variability of fiber orientation with respect to neighboring fibers. A clear difference in color hues were observed from the directional variance heat maps from the two imaging modalities. Scale bars = 50 μ m. B) Quantification of collagen fiber directional variance in the superficial, transitional, and radial zones of the cartilage from SHG (red) and confocal (yellow) imaging. Similar variance maps in the superficial zone were obtained; but those of the other two zones significantly differ between the two imaging methods. For example, in the radial zone, the directional variance peaked at 0.2 from SHG imaging, but peaked at 0.65 from confocal imaging. This indicates that confocal imaging showed more variability of fiber orientation in fibers with their immediate neighbors as compared to SHG imaging. C) Correlation analysis of directional variance from SHG imaging and confocal imaging. No correlation was observed. $p < 0.05$ was considered significant.



Supplemental Figure 7. IHC analysis detecting collagen X protein in knee joints of NF κ B luciferase reporter mouse post-OA induction. A) IHC images of collagen X (Col X) protein at 1-, 3-, 7-, and 10-weeks post-surgery. Hematoxylin was used as a counterstain to indicate nuclei. Scale bar = 400 μ m. B) Negative control for Col X IHC. Mouse knee sections was incubated with secondary antibody (Biotinylated goat anti-rabbit antibody) only. Scale bar = 400 μ m. C) Positive control image of Col X IHC. Col X expression was detected in the hypertrophic chondrocytes in the growth plate of a 3 week-old mouse metatarsal bone. Scale bar = 50 μ m.



Supplemental Fig. 8. Correlation analysis of collagen landscape with cartilage structural damage and synovitis. Data from the Second Harmonic Generation (SHG) imaging on collagen fiber of the tibial plateau were correlated with the Mankin score of the tibia as well as with overall synovitis in NFκB-RE-luc reporter mice after DMM and Sham surgery at 1, 3, 7, and 10 weeks. Spearman's correlation analysis was used. A) Correlation between the ratio of forward and backward SHG signal (FSHG/BSHG) of the deep zone and synovitis. Both the DMM and Sham joints saw an increased FSHG/BSHG signal ratio, which is indicative of collagen fiber thickness, showing a similar trend as synovitis. But upon DMM surgery, there is a shift toward higher synovitis and lower FSHG/BSHG ratio. Red and blue bubbles represent trends in DMM and sham samples respectively. DMM: $r = 0.800$, $p = 0.333$; Sham: $r = 0.600$, $p = 0.417$. B) Correlation between directional variance of the superficial zone fiber and the Mankin score in all samples. Overall, increased variance of collagen fiber is correlated with increased Mankin score for either DMM or Sham samples. $r = 0.926$, $p = 0.002$. Red dots = DMM samples, blue dots = Sham samples.

Supplemental Table 1. Reagents and dilutions for immunohistochemistry

| Target | Antigen Retrieval | Primary Antibody | Secondary Antibody | Stain Development | Counter Stain |
|--------------------|-------------------------------------|---|---|--|--|
| Collagen I | 0.03% hyaluronidase (Sigma Aldrich) | Rabbit anti-Collagen I (AB765P, 1:40 dilution, Sigma Aldrich) | Goat Anti-Rabbit Biotinylated (BA-1000, 1:200 dilution, Vector) | Vectastain Elite ABC kit (Vector); DAB Peroxidase (HRP) subsrate kit (Vector) | Gill's Hematoxlin 1 (Ricca Chemical Company) |
| Collagen II | 0.03% hyaluronidase (Sigma Aldrich) | Rabbit anti-Collagen II (ab34712, 1:50 dilution, Abcam) | Goat Anti-rabbit Alexa594 (A11012, 1:1000, ThermoFisher) | N/A | |
| Collagen X | 0.03% hyaluronidase (Sigma Aldrich) | Rabbit anti-Collagen X (234196, 1:200 dilution, Calbiochem) | Goat Anti-Rabbit Biotinylated (BA-1000, 1:100 dilution, Vector) | Vectastain Elite ABC kit (Vector); DAB Peroxidase (HRP) subsrate kit (Vector) | Gill's Hematoxlin 1 (Ricca Chemical Company) |
| Macrophage | 1% proteinase K (Sigma Aldrich) | Rat anti-F4/80 (Cl:A3-1, 1:150 dilution, BioRad) | Goat Anti-Rat Biotinylated (BA-1000, 1:500 dilution, Vector) | Vectastain Elite ABC kit (Vector) ; DAB Peroxidase (HRP) subsrate kit (Vector) | Gill's Hematoxlin 1 (Ricca Chemical Company) |